The Circumstellar Environments of Young Stars at AU Scales

Rafael Millan-Gabet
California Institute of Technology

Fabien Malbet
Laboratoire d'Astrophysique de Grenoble

Rachel Akeson
California Institute of Technology

Christoph Leinert
Max-Planck-Institut für Astronomie

John Monnier
University of Michigan

Rens Waters
University of Amsterdam

We review recent advances in our understanding of the innermost regions of the circumstellar environment around young stars, made possible by the technique of long baseline interferometry at infrared wavelengths. Near-infrared observations directly probe the location of the hottest dust. The characteristic sizes found are much larger than previously thought, and strongly correlate with the luminosity of the central young stars. This relation has motivated in part a new class of models of the inner disk structure. The first mid-infrared observations have probed disk emission over a larger range of scales, and spectrally resolved interferometry has for the first time revealed mineralogy gradients in the disk. These new measurements provide crucial information on the structure and physical properties of young circumstellar disks, as initial conditions for planet formation.

1. INTRODUCTION

Stars form from collapsing clouds of gas and dust and in their earliest infancies are surrounded by complex environments that obscure our view at optical wavelengths. As evolution proceeds, a stage is revealed with three main components: the young star, a circumstellar disk and an infalling envelope. Eventually, the envelope dissipates, and the emission is dominated by the young star-disk system. Later on, the disk also dissipates to very tenuous levels. It is out of the young circumstellar disks that planets are expected to form, and therefore understanding their physical conditions is necessary before we can understand the formation process. Of particular interest are the inner few AU (Astronomical Unit), corresponding to formation sites of Terrestrial type planets, and to migration sites for gas giants presumably formed further out in the disk (see the chapter by *Udry, Fisher and Queloz*).

A great deal of direct observational support exists for the scenario outlined above, and in particular for the existence of circumstellar disks around young stars (see the chapters by *Dutrey et al.* and by *Watson et al.*). In addition, the spectroscopic and spectro-photometric characteristics of these systems (i.e. spectral energy distributions, emission lines) are also well described by the disk hypothesis. However, current optical and millimeter-wave imaging typically probe scales of $100-1000$s of AU with resolutions of 10s of AU, and models of unresolved observations are degenerate with respect to the spatial distribution of material. As a result, our understanding of even the most general properties of the circumstellar environment at few AU or smaller spatial scales is in its infancy.

Currently, the only way to achieve sufficient angular resolution to directly reveal emission within the inner AU is through interferometry at visible and infrared wavelengths, here referred to as *optical* interferometry. An interferometer with a baseline length of $B = 100$ m (typical of current facilities) operating at near to mid-infrared wavelengths (NIR, MIR, typically H to N bands, $\lambda_0 = 1.65 - 10\,\mu m$) probes $1800 - 300$ K material and achieves an angular resolution $\sim \lambda_0/2B \sim 2 - 10$ milliarcseconds (mas), or $0.25-1.5$ AU at a distance typical of the nearest well known star forming regions (150 pc). This observational discovery

space is illustrated in Fig. 1, along with the domains corresponding to various young stellar object (YSO) phenomena and complementary techniques and instruments. Optical interferometers are ideally suited to directly probe the innermost regions of the circumstellar environment around young stars, and indeed using this technique surprising and rapid progress has been made, as the results reviewed in this chapter will show.

Optical, as well as radio, interferometers operate by coherently combining the electromagnetic waves collected by two or more telescopes. Under conditions that apply to most astrophysical observations, the amplitude and phase of the resulting interference patterns (components of the complex *visibility*) are related via a two-dimensional Fourier transform to the brightness distribution of the object being observed. For a detailed description of the fundamental principles, variations in their practical implementation, and science highlights in a variety of astrophysics areas we refer to the reviews by *Monnier* (2003) and *Quirrenbach* (2001). The reader may also be interested in consulting the proceedings of topical summer schools and workshops such as *Lawson* (2000), *Perrin and Malbet* (2003), *Garcia et al.* (2003) and *Paresce et al.* (2006) (online proceedings of the Michelson Summer Workshops may also be found at `http://msc.caltech.edu/michelson/`).

While interferometers are capable of model-independent imaging by combining the light from many telescopes, most results to date have been obtained using two-telescopes (a single-baseline). The main characteristics of current facilities involved in these studies are summarized in Table 1. Interferometer data, even with sparse spatial frequency coverage, provides direct constraints about source geometry and thus contains some of the power of direct imaging. However, with such data alone only the simplest objects can be constrained. Therefore, more typically, a small number of fringe visibility amplitude data points are combined with a spectral energy distribution (SED) for fitting simple physically-motivated geometrical models; such as a point source representing the central star surrounded by a Gaussian or ring-like brightness (depending on the context) representing the source of infrared excess flux. This allows us to determine "characteristic sizes" at the wavelength of observation for many types of YSOs (e.g., T Tauri, Herbig Ae/Be, FU Orionis). The interferometer data can also can be compared to predictions of specific physical models and this exercise has allowed to rule out certain classes of models, and provided crucial constraints to models that can be made to reproduce the spectral and spatial observables.

A note on nomenclature: Before the innermost disk regions could be spatially resolved, as described in this review, disk models were tailored to fit primarily the unresolved spectro-photometry. The models used can be generally characterized as being geometrically thin and optically thick, with simple radial temperature power laws with exponents $q = -0.75$ (flat disk heated by accretion and/or stellar irradiation, *Lynden-Bell and Pringle*, 1974) or shallower (flared disks, *Kenyon and Hartmann*, 1987; *Chiang and Goldreich*, 1997). In this review, we will refer to these classes of models as "classical", to be distinguished from models with a modified inner disk structure that have recently emerged in part to explain the NIR interferometer measurements.

The outline of this review is as follows. Sections 2 and 3 summarize the observational state of the art and emerging interpretations, drawing a physically motivated distinction between inner and outer disk regions that also naturally addresses distinct wavelength regimes and experimental techniques. We note that these developments are indeed recent, with the first preliminary analyses of interferometric observations of YSOs being presented (as posters) at the Protostars and Planets IV Conference in 1998. In Section 4 we highlight additional YSO phenomena that current facilities are addressing, such as the disk-wind connection and young star mass determination, using combination of interferometry with high resolution line spectroscopy. In Section 5 we present a top-level summary of the main well-established results, and highlight remaining important open questions likely to be experimentally and theoretically addressed in the coming years. In Section 6 we describe additional phenomena yet to be explored and new instrumental capabilities that promise to enable this future progress.

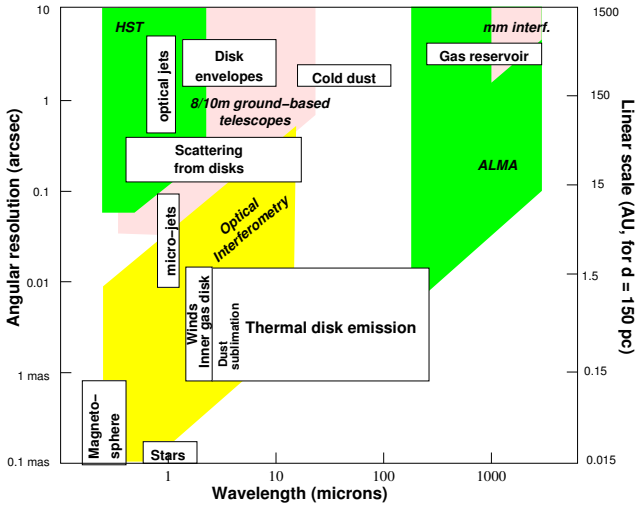

Fig. 1.— Observational phase-space (spectral domain and angular resolution) for optical interferometers, and for complementary techniques (shaded polygons). Also outlined over the most relevant phase-space regions (rectangular boxes) are the main physical phenomena associated with young stellar objects.

2. THE INNER DISK

At NIR wavelengths ($\sim 1 - 2.4\,\mu m$) optical interferometers probe the hottest circumstellar material located at stellocentric distances $\lesssim 1$ AU. In this review these regions are referred to as the *inner disk*. For technical reasons, it is at NIR wavelengths that interferometric measurements of YSOs first became possible, and provided the first direct probes of inner disk properties. Until only a few years ago,

TABLE 1
LONG BASELINE OPTICAL INTERFEROMETERS INVOLVED IN YSO RESEARCH

Facility	Instrument[a]	Wavelength Coverage[b]	Number of Telescopes[c]	Telescope Diameter (m)	Baseline Range (m)	Best Resolution[d] (mas)
PTI	V^2	$1.6-2.2\mu m$ [44]	2 [3]	0.4	$80-110$	1.5
IOTA	V^2, IONIC3	$1.6-2.2\mu m$	3	0.4	$5-38$	4.5
ISI	Heterodyne	$11\mu m$	3	1.65	$4-70$	16.2
KI	V^2	$1.6-2.2\mu m$ [22]	2	10	85	2.0
KI	Nuller	$8-13\mu m$ [34]	2	10	85	9.7
VLTI	MIDI	$8-13\mu m$ [250]	2 [8]	8.2 / 1.8	$8-200$	4.1
VLTI	AMBER	$1-2.5\mu m$ [10^4]	3 [8]	8.2 / 1.8	$8-200$	0.6
CHARA	V^2	$1.6-2.2\mu m$	2 [6]	1	$50-350$	0.4

NOTE.—**(a)** V^2 refers to a mode in which only the visibility amplitude is measured, often implemented in practice as a measurement of the (un-biased estimator) square of the visibility amplitude. **(b)** The maximum spectral resolution available is given in square brackets. **(c)** The number of telescopes that can be simultaneously combined is given, along with the total number of telescopes available in the array in square brackets. **(d)** In each case, the best resolution is given as half the fringe spacing, $\lambda_{min}/(2B_{max})$, for the longest physical baseline length and shortest wavelength available. **References:** [1] PTI, *Palomar Testbed Interferometer, Colavita et al* 1999. [2] IOTA, *Infrared-Optical Telescope Array, Traub et al.* 2004. [3] ISI, *Infrared Spatial Interferometer, Hale et al.* 2000. [4] KI, *Keck Interferometer, Colavita, Wizinovich and Akeson* 2004. [5] KI Nuller, *Serabyn et al.* 2004. [6] MIDI, *MID-infrared Interferometric instrument, Leinert et al.* 2003. [7] AMBER, *Astronomical Multiple BEam Recombiner, Malbet et al.* 2004. [8] CHARA, *Center for High Angular Resolution Astronomy interferometer, ten Brummelaar et al.* 2005.

relatively simple models of accretion disks were adequate to reproduce most observables. However, the new observations with higher spatial resolution have revealed a richer set of phenomena.

2.1 Herbig Ae/Be Objects

In Herbig Ae/Be (HAeBe) objects, circumstellar material (proto-planetary disk, remnant envelope, or both) surrounds a young star of intermediate mass ($\sim 2-10\,M_\odot$, see e.g., the review by *Natta et al.* 2000). A significant number of these objects fall within the sensitivity limits of small interferometers, hence the first YSO studies containing relatively large samples focused on objects in this class.

AB Aur was the first "normal" (i.e. non-outburst, see Section 2.3) YSO to be resolved at NIR wavelengths. In observations at the *Infrared Optical Telescope Array* (IOTA) AB Aur appeared clearly resolved in the H and K spectral bands on 38 m baselines, by an amount corresponding to a characteristic diameter of 0.6 AU for the circumstellar NIR emission (*Millan-Gabet et al.*, 1999). The measured size was unexpectedly large in the context of then-current disk models of HAeBe objects (e.g., *Hillenbrand et al.*, 1992) which predicted NIR diameter of 0.2 AU based on optically-thick, geometrically-thin circumstellar disk with a small dust-free inner hole. This conclusion was reinforced by the completed IOTA survey of *Millan-Gabet et al.* (2001), finding characteristic NIR sizes of 0.6−6 AU for objects with a range of stellar properties (spectral types A2–O9).

Due to the limited position angle coverage of these first single-baseline observations, the precise geometry of the NIR emission remained ambiguous. *Millan-Gabet et al.* (2001) found that the NIR sizes were similar at 1.65 and $2.2\,\mu m$, suggesting a steep temperature gradient at the inner disk edge. These early observations revealed no direct evidence for "disk-like" morphologies; indeed, for the few objects with size measurements at multiple position angles, the data indicated circular symmetry (as if from spherical halos or face-on disks, but not inclined disks).

The first unambiguous indication that the NIR emission arises in disk-like structures came from single-telescope imaging of the highly-luminous YSOs LkHα 101 and MWC 349-A, using a single-telescope interferometric technique (aperture masking at the Keck I telescope). MWC 349-A appeared clearly elongated (*Danchi et al.*, 2001) and LkHα 101 presented an asymmetric ring-like morphology, interpreted as a bright inner disk edge occulted on one side by foreground cooler material in the outer regions of the flared disk (*Tuthill et al.*, 2001). Moreover, the location of the LkHα 101 ring was also found to be inconsistent with predictions of classical disk models and these authors suggested that an optically-thin inner cavity (instead of optically-thick disk midplane) would result in larger dust sublimation radii, consistent with the new size measurements.

Could simple dust sublimation of directly heated dust be setting the NIR sizes of other HAeBe objects as well? The idea was put to the test by *Monnier and Millan-*

Gabet (2002). Inspired by the LkHα 101 morphology and interpretation, these authors fit a simple model consisting of a central star surrounded by a thin ring for all objects that were measured interferometrically at the time (IOTA and aperture masking, plus first YSO results from the *Palomar Testbed Interferometer*, PTI, *Akeson et al.*, 2000). Indeed, the fitted ring radii are clearly correlated with the luminosity of the central star, and follow the expected relation $R \propto L_\star^{1/2}$. Further, by using realistic dust properties it was also found that the measured NIR sizes are consistent with the dust sublimation radii of relatively large grains ($\gtrsim 1\,\mu m$) with sublimation temperatures in the range 1000 K$-$2000 K.

Following *Monnier and Millan-Gabet* (2002), in Fig. 2 we have constructed an updated diagram of NIR size *vs.* central luminosity based on all existing data in the literature. We include data for both HAeBe and T Tauri objects, the latter being discussed in detail in the next Section; and we also illustrate schematically the essential ingredients (i.e. location of the inner dust disk edge) of the models to which the data are being compared. For HAeBe objects, disk irradiation is dominated by the stellar luminosity, and therefore we neglect heating by accretion shock luminosity (which may play a significant role for the most active lower stellar luminosity T Tauri objects, as discussed in the next section).

Indeed, it can be seen that for HAe and late HBe objects, over more than two decades in stellar luminosity, the measured NIR sizes are tightly contained within the sublimation radii of directly heated grey dust with sublimation temperatures of 1000 K$-$1500 K under the assumption that dust grains radiate over the full solid angle (e.g., no backwarming, solid lines in Fig. 2). If instead we assume that the dust grains emit only over 2π steradian (e.g., full backwarming) then the corresponding sublimation temperature range is 1500 K$-$2000 K.

The most luminous objects (the early spectral type HBe objects) on the other hand, have NIR sizes in good agreement with the classical model, indicating that for these objects the disk extends closer in to the central star. *Monnier and Millan-Gabet* (2002) hypothesized that even optically thin low-density gas inside the dust destruction radius can scatter UV stellar photons partly shielding the dust at the inner disk edge and reducing the sublimation radius. *Eisner et al.* (2003, 2004) argue instead that the distinction may mark a transition from magnetospheric accretion (late types) to a regime for the early types where optically-thick disks in fact do extend to the stellar surface, either as a result of higher accretion rates or weak stellar magnetic fields. We note that using polarimetry across H_α lines originating in the inner gas disk at $\sim$ few $R_\star$, *Vink et al.* (2005) (and references therein) also find (in addition to flattened structures consistent with disk-like morphology) a marked difference in properties between HBe objects and HAe and T Tauri objects; qualitatively consistent with the NIR size properties described above. However, not *all* high luminosity HBe objects are in better agreement with the classical model; there are notable exceptions (e.g., LkHα 101, MWC 349-A, see Fig. 2) and *Monnier et al.* (2005a) have noted that these may be more evolved systems, where other physical processes, such as dispersal by stellar winds or erosion by photo-evaporation, have a dominant effect in shaping the inner disk.

In parallel with these developments, and in the context of detailed modelling of the NIR SED, *Natta et al.* (2001) similarly formulated the hypothesis that the inner regions of circumstellar disks may be largely optically thin to the stellar photons such that a directly illuminated "wall" forms at the inner dust-disk edge. The relatively large surface area of this inner dust wall is able to produce the required levels of NIR flux (the so-called NIR SED "bump"). The simple blackbody surface of the initial modelling implementation has since been replaced by more realistic models which take additional physical effects into account: self-consistent treatment of radiative transfer and hydrostatic vertical structure of the inner wall and corresponding outer disk shadowing (*Dullemond et al.*, 2001), optical depth and scale height of gas inside the dust destruction radius (*Muzerolle et al.*, 2004), and inner rim curvature due to density-dependent dust sublimation temperature (*Isella and Natta*, 2005).

Independent of model details however, it is clear that the optically-thin cavity disk model with a "puffed-up" inner dust wall can explain a variety of observables: the ring-like morphology, the characteristic NIR sizes and the NIR SED. We also emphasize that although the discussion of the interferometer data presented above was centered around the size-luminosity diagram, the same conclusions have been obtained by modelling SEDs and visibility measurements for individual sources using physical models of both classical and puffed-up inner rim models.

Although the characteristic NIR sizes have now been well established for a relatively large sample, few constraints still exist as to the actual geometry of the resolved NIR emission. In this respect, most notable are the PTI observations of *Eisner et al.* (2003, 2004) which provided the first evidence for elongated emission, consistent with inclined disks. Further, the inclinations found can explain the residual scatter (50%) in the size-luminosity relation for HAe and late HBe systems (*Monnier et al.*, 2005a).

It is important to note that three different interferometers have now reached the same conclusions regarding the characteristic NIR sizes of HAeBe objects, in spite of having vastly different field-of-views (FOV; 3, 1, and 0.05 *arcsec* FWHM for IOTA, PTI and KI respectively). This indicates that the interpretation is not significantly effected by non-modelled flux entering the FOV, from the large scale (scattered) emission often found around these objects (e.g., *Leinert et al.*, 2001). Indeed, if not taken into account in a composite model, such incoherent flux would lead to overestimated characteristic sizes, and still needs to be considered as a (small) possible effect for some objects.

2.2 T Tauri Objects

Only the brightest T Tauri objects can be observed with the small aperture interferometers, so early observations were limited in number. The first observations were taken at the PTI and were of the luminous sources T Tau N and SU Aur (*Akeson et al.*, 2000, 2002). Later observations (*Akeson et al.*, 2005a) added DR Tau and RY Tau to the sample, and employed all three PTI baselines to constrain the disk inclination. Using simple geometrical models (or simple power-law disk models) the characteristic NIR sizes (or disk inner radii) were found to be larger than predicted by SED-based models (*e.g., Malbet and Bertout*, 1995), similar to the result for the HAe objects. For example, inclined ring models for SU Aur and RY Tau yield radii of 10 $R_\star$ and 11 $R_\star$ respectively, substantially larger than magnetic truncation radii of 3–5 $R_\star$ expected from magnetospheric accretion models (*Shu et al.*, 1994). If the inner dust disk does not terminate at the magnetic radius, what then sets its radial location? Interestingly, these initial T Tauri observations revealed NIR sizes that were also consistent with sublimation radii of dust directly heated by the central star, suggesting perhaps that similar physical processes, decoupled from magnetospheric accretion, set the NIR sizes of both T Tauri and HAe objects. *Lachaume et al.* (2003) were the first to use physical models to fit the new visibility data, as well as the SEDs. Using a two-layer accretion disk model, these authors find satisfactory fits for SU Aur (and FU Ori, see Section 2.3), in solutions that are characterized by the mid-plane temperature being dominated by accretion, while the emerging flux is dominated by reprocessed stellar photons.

Analysis of T Tauri systems of more typical luminosities became possible with the advent of large aperture infrared interferometers. Observations at the KI (*Colavita et al.*, 2003; *Eisner et al.*, 2005; *Akeson et al.*, 2005a) continued to find large NIR sizes for lower luminosity stars, in many cases even larger than would be expected from extrapolation of the HAe relation.

Current T Tauri measurements and comparison with dust sublimation radii are also summarized in Fig. 2. *Eisner et al.* (2005) found better agreement with puffed-up inner wall models, and in Fig. 2 we use their derived inner disk radii. Following *Muzerolle et al.* (2003) and *D'Alessio et al.* (2004), the central luminosity for T Tauri objects includes the accretion luminosity, released when the magnetic accretion flow encounters the stellar surface, which can contribute to the location of the dust sublimation radius for objects experiencing the highest accretion rates (in Fig. 2, accretion luminosity only affects the location of three objects significantly: AS205–A, PX Vul and DR Tau, having $L_{accretion}/L_\star \sim 10.0, 1.8, 1.2$ respectively.)

It can be seen that many T Tauri objects follow the HAe relation, although several are even larger given the central luminosity (the T Tauri objects located above the 1000 K solid line in Fig. 2 are: BP Tau, GM Aur, LkCa 15 and RW Aur).

It must be noted however that current measurements of the lowest luminosity T Tauri objects have relatively large errors. Further, the ring radii plotted in Fig. 2 depend on the relative star/disk NIR flux contributions, most often derived from an SED decomposition which for T Tauri objects is considerably more uncertain than for the HAeBe objects, due to their higher photometric variability, and the fact that the stellar SEDs peak not far ($\sim 1\,\mu m$) from the NIR wavelengths of observation. We note that an improved approach was taken by *Eisner et al.* (2005), who derived stellar fluxes at the KI wavelength of observation from near contemporaneous optical veiling measurements and extrapolation to NIR wavelengths based on model atmospheres. These caveats illustrate the importance of obtaining more direct estimates of the excess NIR fluxes, via veiling measurements (e.g., *Johns-Krull and Valenti*, 2001 and references therein).

Under the interpretation that the T Tauri NIR sizes trace the dust sublimation radii, different properties for the dust located at the disk inner edge appear to be required to explain all objects. In particular, if the inner dust-disk edge becomes very abruptly optically thick (e.g., strong backwarming), the sublimation radii become larger by a factor of $\times 2$, in better agreement with some of the low luminosity T Tauri objects (dashed lines in Fig. 2). As noted by *Monnier and Millan-Gabet* (2002), smaller grains also lead to larger sublimation radii, by a factor $\sqrt{Q_R}$, where Q_R is the ratio of dust absorption efficiencies at the temperatures of the incident and re-emitted field ($Q_R \simeq 1 - 10$ for grain sizes $1.0 - 0.03\,\mu m$, the incident field of a stellar temperature of 5000 K typical of T Tauri stars, and re-emission at 1500 K).

Alternatively, an evolutionary effect could be contributing to the size-luminosity scatter for the T Tauri sample. *Akeson et al.* (2005a) note that the size discrepancy (measured *vs.* sublimation radii) is greatest for objects with the lowest ratio of accretion to stellar luminosity. If objects with lower accretion rates are older (e.g., *Hartmann et al.*, 1998) then other physical processes such as disk dispersal (*Clarke et al.*, 2001, see also the review by *Hollenbach et al.*, 2000) may be at play for the most "discrepant" systems mentioned above (the size derived for GM Aur contains additional uncertainties, given the evidence in this system for a dust gap at several AU, *Rice et al.*, 2003, and the possibility that it contributes significant scattered NIR light).

In detailed modelling work of their PTI data, *Akeson et al.* (2005b) used Monte Carlo radiative transfer calculations (*Bjorkman and Wood*, 2001) to model the SEDs and infrared visibilities of SU Aur, RY Tau and DR Tau. These models addressed two important questions concerning the validity of the size interpretation based on fits to simple star + ring models: (1) Is there significant NIR thermal emission from *gas* inside the dust destruction radius? and, (2) is there significant flux arising in large scale (scattered) emission? The modelling code includes accretion and shock/boundary luminosity as well as multiple scattering and this technique naturally accounts for the radiative transfer effects and the heating and hydrostatic structure of the inner wall of the disk. In these models, the gas disk

extends to within a few stellar radii and the dust disk radius is set at the dust sublimation radius. For SU Aur and RY Tau, the gas within the inner dust disk was found to contribute substantially to the NIR emission. Modelling of HAeBe circumstellar disks by *Muzerolle et al.* (2004) found that emission from the inner gas exceeded the stellar emission for accretion rates $> 10^{-7}$ $M_\odot$ yr^{-1}. Thus, even as a simple geometrical representation, a ring model at the dust sublimation temperature may be too simplistic for sources where the accretion luminosity is a substantial fraction of the total system luminosity. Moreover, even if the NIR gas emission were located close to the central star and were essentially unresolved, its presence would affect the SED decomposition (amount of NIR excess attributed to the dust "ring"), leading to incorrect (under-estimated) ring radii. The second finding from the radiative models is that the extended emission (here meaning emission from scales larger than 10 mas) was less than 6% of the total emission for all sources, implying that scattered light is not a dominant component for these systems.

Clearly, the new spatially resolved observations just described, although basic, constitute our only direct view into the physical conditions in young disks on scales $\lesssim 1$ AU, and therefore deliver crucial ingredients as pre-conditions for planet formation. As pointed out by *Eisner et al.* (2005) the interpretation that the measured NIR sizes correspond to the location of the innermost disk dust implies that dust is in fact present at Terrestrial planet locations. Conversely, the measured radii imply that no dust exists, and therefore planet formation is unlikely, inside these relatively large $\sim$ 0.1–1 AU inner dust cavities. Finally, that the dust disk stops at these radii may also have implications for planet migration, depending on whether migration is halted at the inner radius of the gas (*Lin et al.*, 1996) or dust (*Kuchner and Lecar*, 2002) disk (see also the chapter by *Papaloizou et al.*).

2.3 Detailed Tests of the Disk Hypothesis: FU Orionis

FU Orionis objects are a rare type of YSO believed to be T Tauri stars surrounded by a disk that has recently undergone an episode of accretion rate outburst (see e.g., the review by *Hartmann et al.*, 1996). During the outburst, the system brightens by several visual magnitudes, followed by decade-long fading. The disk luminosity dominates the emission at all wavelengths, and is expected to be well represented by thermal emission by disk annulii that follow the canonical temperature profile $T \propto r^{-3/4}$. With this prescription, the model has few parameters that are well constrained by the SEDs alone (except for inclination effects). In principle then, these systems are ideal laboratories for testing the validity of disk models. The total number of known objects in this class is small (e.g., 20 objects in the recent compilation by *Ábrahám et al.*, 2004), and the subset that is observable by current optical interferometers is even smaller (about 6 objects, typically limited by instrumental sensitivity at short wavelengths $0.55 - 1.25\,\mu m$).

The very first YSO to be observed with an optical interferometer was in fact the prototype for this class, FU Orionis itself (*Malbet et al.*, 1998). Indeed, the first K-band visibility amplitudes measured by the PTI agreed well with the predictions of the canonical disk model. This basic conclusion has been re-inforced in a more recent study using multi-baseline, multi-interferometer observations (*Malbet et al.*, 2005). The detailed work on FU Ori will ultimately close the debate on its nature: current evidence favors that it is a T Tauri star surrounded by a disk undergoing massive accretion (*Hartmann and Kenyon*, 1985, 1996) rather than a rotating supergiant with extreme chromosphere activity (*Herbig et al.*, 2003); and under that interpretation the physical (temperature law) and geometrical (inclination and orientation) parameters describing the disk have been established with unprecedented detail.

Three more FU Orionis objects have been resolved in the NIR: V1057 Cyg (PTI, *Wilkin and Akeson*, 2003; KI *Millan-Gabet et al.*, 2006), V1515 Cyg and ZCMa-SE (*Millan-Gabet et al.*, 2006). In contrast to the FU Ori case, these three objects appear more resolved in the NIR than expected from a $T \propto r^{-3/4}$ model, and simple exponent adjustments of such a single power-law model does not allow simultaneous fitting of the visibilities and SEDs. On the other hand, these objects are also known to possess large mid-infrared fluxes in excess of emission by flat disks, usually attributed to a large degree of outer disk flaring or, more likely, the presence of a dense dust envelope (*Kenyon and Hartmann*, 1991). The low visibilities measured, particularly for V1057 Cyg and V1515 Cyg, can be explained by K-band flux ($\sim$ 10% of total) in addition to the thermal disk emission, resulting from scattering through envelope material over scales corresponding to the interferometer FOV (50 mas FWHM). Contrary to initial expectations, the likely complexity of the circumstellar environment of most FU Orionis objects will require observations at multiple baselines and wavelengths in order to disentangle the putative multiple components, discriminate between the competing models, and perform detailed tests of accretion disk structure.

3. THE OUTER DISK

At mid-infrared (MIR) wavelengths, and for $50-100$ m baselines, optical interferometers probe the spatial distribution and composition of $\sim$ few 100 K circumstellar gas and dust, with $8-27$ mas resolution, or $1-4$ AU at a distance of 150 pc. The MIR radiation of circumstellar disks in the N-band ($8 - 13\,\mu m$) comes from a comparatively wide range of distances from the star, see Fig. 3, and we now focus the discussion on circumstellar dust in this several-AU transition region between the hottest dust in the sublimation region close to the star (Section 2), and the much cooler disk regions probed by mm interferometry (see the chapter by *Dutrey et al.*) and by scattered light imaging (see the chapter by *Watson et al.*). As a matter of interpretational convenience, at these longer MIR wavelengths the flux contri-

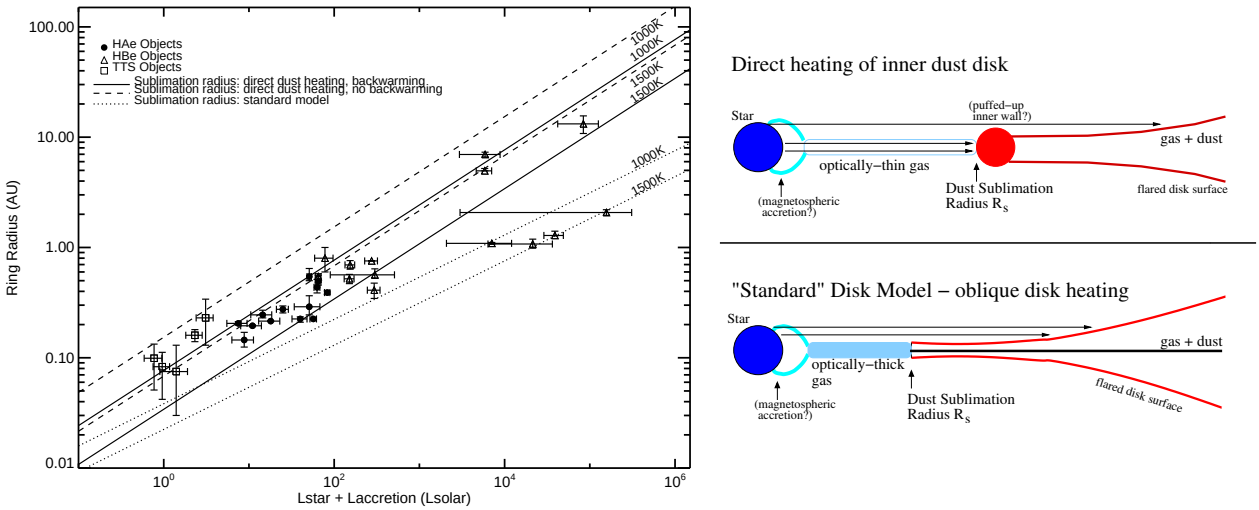

Fig. 2.— Measured sizes of HAeBe and T Tauri objects *vs.* central luminosity (stellar + accretion shock); and comparison with sublimation radii for dust directly heated by the central luminosity (solid and dashed lines) and for the oblique heating implied by the classical models (dotted line). A schematic representation of the key features of inner disk structure in these two classes of models is also shown. Data for HAeBe objects are from: IOTA (*Millan-Gabet et al.*, 2001), Keck aperture masking (*Danchi et al.*, 2001, *Tuthill et al.*, 2001), PTI (*Eisner et al.*, 2004) and KI (*Monnier et al.*, 2005a). Data for T Tauri objects are from PTI (*Akeson et al.*, 2005b) and KI (*Akeson et al.*, 2005a, *Eisner et al.*, 2005). For clarity, for objects observed at more than one facility, we include only the most recent measurement.

bution from scattered light originating from these relatively small spatial scales is negligible, allowing to consider fewer model components and physical processes.

3.1 Disk Sizes and Structure

The geometry of proto-planetary disks is of great importance for a better understanding of the processes of disk evolution, dissipation and planet formation. The composition of the dust in the upper disk layers plays a crucial role in this respect, since the optical and UV photons of the central star, responsible for determining the local disk temperature and thus the disk vertical scale-height, are absorbed by these upper disk layer dust particles. The disk scale-height plays a pivotal role in the process of dust aggregation and settling, and therefore impacts the global disk evolution. In addition, the formation of larger bodies in the disk can lead to structure, such as density waves and gaps.

Spatially resolved observations of disks in the MIR using single telescopes have been limited to probing relatively large scale (100s AU) thermal emission in evolved disks around main-sequence stars (e.g., *Koerner et al.*, 1998; *Jayawardhana*, 1998) or scattering by younger systems (e.g., *McCabe et al.*, 2003). Single-aperture interferometric techniques (e.g., nulling, *Hinz et al.*, 2001; *Liu et al.*, 2003, 2005 or segment-tilting, *Monnier et al.*, 2004b) as well as observations at the *Infrared Spatial Interferometer* (ISI, *Tuthill et al.*, 2002) have succeeded in resolving the brightest young systems on smaller scales for the first time, establishing MIR sizes of $\sim$ 10s AU. Although the observed samples are still small, and thus far concern mostly HAe objects, these initial measurements have already provided a number of interesting, albeit puzzling results: MIR characteristic sizes may not always be well predicted by simple (flared) disk models (some objects are "under-sized" compared to these predictions, opposite to the NIR result), and may not always connect in a straightforward way with measurements at shorter (NIR) and longer (mm) wavelengths.

These pioneering efforts were however limited in resolution (for the single-aperture techniques) or sensitivity (for the heterodyne ISI), and probing the MIR emission on small scales has only recently become possible with the advent of the new-generation long baseline MIR instruments (VLTI/MIDI, *Leinert et al.*, 2003; KI/Nuller, *Serabyn et al.*, 2004).

Two main factors determine the interferometric signature of a dusty protoplanetary disk in the MIR: The overall geometry of the disk, and the composition of the dust in the disk "atmosphere." The most powerful way to distentangle these two effects is via spectrally resolved interferometry, and this is what the new generation of instruments such as MIDI at the VLTI are capable of providing.

First results establishing the MIR sizes of young circumstellar disks were obtained by VLTI/MIDI for a sample of seven HAeBe objects (*Leinert et al.* 2004). The characteristic sizes measured, based on visibilities at the wavelength of $12.5\,\mu m$, are in the range 1–10 AU. Moreover, as shown in Fig. 4, they are found to correlate with the IRAS [12]–[25] color, with redder objects having larger MIR sizes. These observations lend additional support to the SED-based classification of *Meeus et al.* (2001) and *Dullemond and Dominik* (2004), whereby redder sources correspond to disks with a larger degree of flaring, which therefore also emit

thermally in the MIR from larger radii, compared to sources with flatter disks.

A more powerful analysis is possible by exploiting the spectral resolution capabilities of the MIDI instrument. Based on the reddest object in the *Leinert et al.* 2004 sample (HD 100546), the spectrally resolved visibilities also support the *Meeus et al.* (2001) classification: this object displays a markedly steeper visibility drop between $8-9\,\mu m$, and lower visibilities at longer wavelengths than the rest of the objects in the sample, implying the expected larger radius for the MIR emission. These first observations have also been used to test detailed disk models that were originally synthesized to fit the SEDs of individual objects (*Dominik et al.*, 2003); without any feedback to the models *Leinert et al.* (2004) find encouraging qualitative agreement between the predicted spectral visibility shapes and the interferometer data.

It remains to be seen whether direct fitting to the interferometer data will solve the remaining discrepancies (see e.g., the work of *Gil et al.*, 2005 on the somewhat unusual object 51 Oph) . In general, changes in both disk geometry and dust composition strongly affect the MIR spectral visibilities. However simulations by *van Boekel et al.* (2005) have shown that the problem is tractable and even just a few well-chosen baselines (and wavelengths) permit a test of some of the key features of recently proposed disk models, such as the presence of the putative puffed-up inner rim and the degree of outer disk flaring (which in these models is influenced by shadowing by the inner rim).

Clearly, the spectrally and spatially resolved disk observations made possible by instruments such as VLTI/MIDI will prove crucial towards further exploring exciting prospects for linking the overall disk structure, the properties of midplane and surface layer dust, and their time evolution towards the planet-building phase (see also the chapter by *Dominik et al.*).

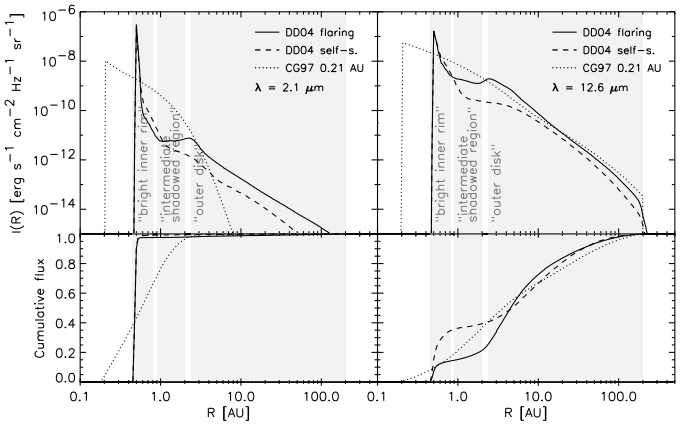

Fig. 3.— Predicted radial distribution of NIR (left) and MIR (right) light for typical disk models. DD04 (*Dullemond and Dominik*, 2004) refers to a 2D radiative transfer and hydrostatic equilibrium Monte Carlo code featuring a puffed up inner rim; CG97 to the gradually flaring model of *Chiang and Goldreich* 1997. We note that the CG97 disk model can not self-consistently treat the inner disk once the temperature of the "super-heated" dust layer increases beyond the dust sublimation temperature. This only effects the NIR light profiles and here the disk was artificially truncated at 0.21 AU. The central star is assumed to be of type A0 with M=2.5 $M_\odot$ and R = 2.0 $R_\odot$. The upper panels show the intensity profiles, and the lower panels the cumulative brightness contributions, normalized to 1. Three qualitatively different disk regions are indicated by shadowing. This figure illustrates that NIR observations almost exclusively probe the hot inner rim of the circumstellar disks, while MIR observations are sensitive to disk structure over the first dozen or so AU. (Credit: Roy van Boekel).

3.2 Dust Mineralogy and Mixing

The MIR spectral region contains strong resonances of abundant dust species, both O–rich (amorphous or crystalline silicates) and C–rich (Polycyclic Aromatic Hydrocarbons, or PAHs). Therefore, MIR spectroscopy of optically thick proto-planetary disks offers a rich diagnostic of the chemical composition and grain size of dust in the upper disk layers or "disk atmosphere". At higher spectral resolution, $R \sim$ few 100, gas emission such as [NeII] lines and lines of the Hund and higher hydrogen series can be observed. It should be noted that these observations do not constrain the properties of large ($> 2-4\,\mu m$) grains, since these have little or no spectral structure at MIR wavelengths. In the sub-micron and micron size range however, different silicate particles can be well distinguished on the basis of the shape of their emission features. Clearly, valuable information can be obtained from spatially unresolved observations – the overall SED constrains the distribution of material with temperature (or radius), and MIR spectroscopy provides the properties of dust. However, strong radial gradients in the nature of the dust are expected, both in terms of size and chemistry, that can only be observed with spatially resolved observations.

Van Boekel et al. (2004) have demonstrated the power of spectrally resolved MIR interferometry, by spatially resolving three proto-planetary disks surrounding HAeBe stars across the N-band. The correlated spectra measured by VLTI/MIDI correspond to disk regions at 1–2 AU. By combining these with unresolved spectra, the spectrum corresponding to outer disk regions at 2–20 AU can also be deduced. These observations have revealed radial gradients in dust crystallinity, particle size (grain growth), and at least in one case (HD 142527) chemical composition. These early results have revived the discussion of radial and out-of-the-plane mixing.

Interstellar particles observed in the direction of the galactic center are mainly small amorphous Olivine grains ($Fe_{2-2x}Mg_{2x}SiO_4$) with some admixture of Pyroxene grains ($Fe_{1-x}Mg_xSiO_3$) (*Kemper et al.*, 2004). In our planetary system, comets like Halley, Levi or Hale-Bopp (*Hanner et al.*, 1994; *Crovisier et al.*, 1997) show the features of crystalline Forsterite (an Mg-rich Olivine, x=1), in particular the conspicuous emission at $11.3\,\mu m$.

The VLTI/MIDI observations have revealed that crys-

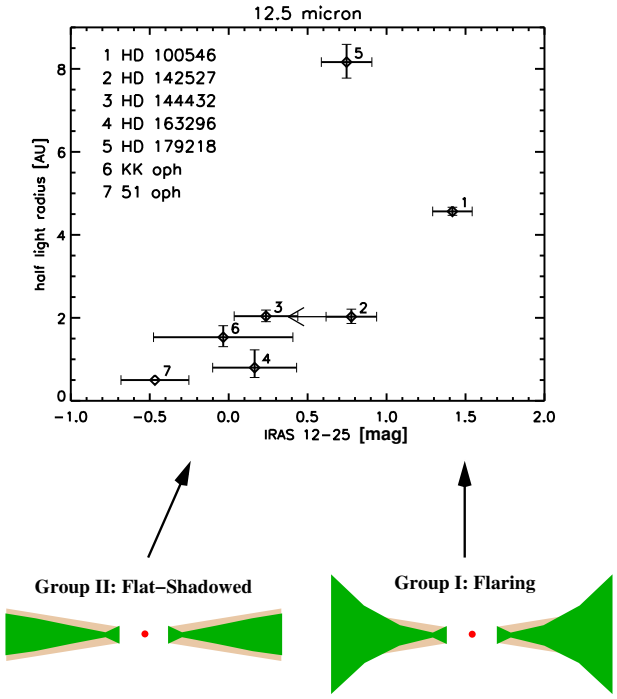

Fig. 4.— Relation between $12.5\ \mu m$ sizes (measured as half-light radius) and infrared slope (measured by IRAS colors) for the first HAeBe stars observed with MIDI on the VLTI. This size-color relation is consistent with expectations from the SED classification of *Meeus et al.* (2001) into objects with flared *vs.* flat outer disks.

tallinization in young circumstellar disks can be a very efficient process, by suggesting a very high fraction of crystalline dust in the central 1–2 AU; and that the outer 2–20 AU disk posseses a markedly lower crystalline fraction, but still much higher than in the interstellar medium. Combined with the very young evolutionary status of these systems (as young as 1 Myr), these observations imply that proto-planetary disks are highly crystalline well before the onset of planet formation. The presence of crystalline dust in relatively cold disk regions (or in Solar System comets) is surprising, given that temperatures in these regions are well below the glass temperature of ~ 1000 K, but can be explained by chemical models of proto-planetary disks that include the effects of radial mixing and local processes in the outer disk (*Gail*, 2004; *Bockelée-Morvan et al.*, 2002). The radial gradient found in dust chemistry is also in qualitative agreement with the predictions of these models. Finally, the width of the silicate feature in the MIDI spectra corresponding to the inner and outer disk have revealed a radial gradient in (amorphous) grain size, with small grains (broader feature) being less abundant in the inner disk regions. This is perhaps expected, given that grain aggregation is a strong function of density (see the chapter by *Natta et al.*). Fig. 5 includes an example illustrating radial dust mineralogy gradients for the HAe object HD 144432.

These radial gradients in dust mineralogy are of course not restricted to HAeBe stars, but are expected in all YSO disks. In Fig. 5 we show preliminary VLTI/MIDI results for two low-mass objects of different evolutionary status, TW Hya and RY Tau (*Leinert and Schegerer*, 2006, in preparation). For TW Hya, the spatially unresolved N-band spectrum (right panel) shows no strong evidence for crystalline silicates, while the correlated flux spectrum (left panel) shows a weak but highly processed silicate band. Preliminary modelling indicates that the inner disk region of TW Hya contains a high fraction of crystalline silicates (30%), and that the amorphous grains have aggregated to larger units. As with the HAeBe stars, not all T Tauri objects show the same features; e.g., the effect is qualitatively similar but quantitatively less pronounced in RY Tau, as can be seen in Fig. 5.

4. OTHER PHENOMENA

4.1 Outflows and Winds

The power of spectrally resolved interferometric measurements has recently become available in the NIR spectral range as well (VLTI/AMBER, *Malbet et al.*, 2004; CHARA/MIRC, *Monnier et al.*, 2004a). In addition to providing the detailed wavelength dependence of inner disk continuum (dust) emission, these capabilities enable detailed studies of the physical conditions and kinematics of the gaseous components in which emission and absorption lines arise (e.g., Br_γ, CO and H_2 lines; as probes of hot winds, disk rotation and outflows, respectively).

As a rather spectacular example of this potential, during its first commissioning observations the VLTI/AMBER instrument spatially resolved the luminous HBe object MWC 297, providing visibility amplitudes as a function of wavelength at intermediate spectral resolution $R = 1500$ across a $2.0 - 2.2\,\mu m$ band, and in particular a finely sampled Br_γ emission line (*Malbet et al.*, 2006). The interferometer visibilities in the Br_γ line are $\sim 30\%$ lower than those of the nearby continuum, showing that the Br_γ emitting region is significantly larger than the NIR continuum region.

Known to be an outflow source (*Drew et al.*, 1997), a preliminary model has been constructed by *Malbet et al.* (2006) in which a gas envelope, responsible for the Br_γ emission, surrounds an optically thick circumstellar disk (the characteristic size of the line emitting region being 40% larger than that of the NIR disk). This model is successful at reproducing the new VLTI/AMBER measurements as well as previous continuum interferometric measurements at shorter and longer baselines (*Millan-Gabet et al.*, 2001; *Eisner et al.*, 2004), the SED, and the shapes of the H_α, H_β and Br_γ emission lines.

The precise nature of the MWC 297 wind however remains unclear; the limited amount of data obtained in these first observations can not, for example, discriminate between a stellar or disk origin for the wind, or between competing models of disk winds (e.g., *Casse and Ferreira*, 2000; *Shu et al.*, 1994). These key questions

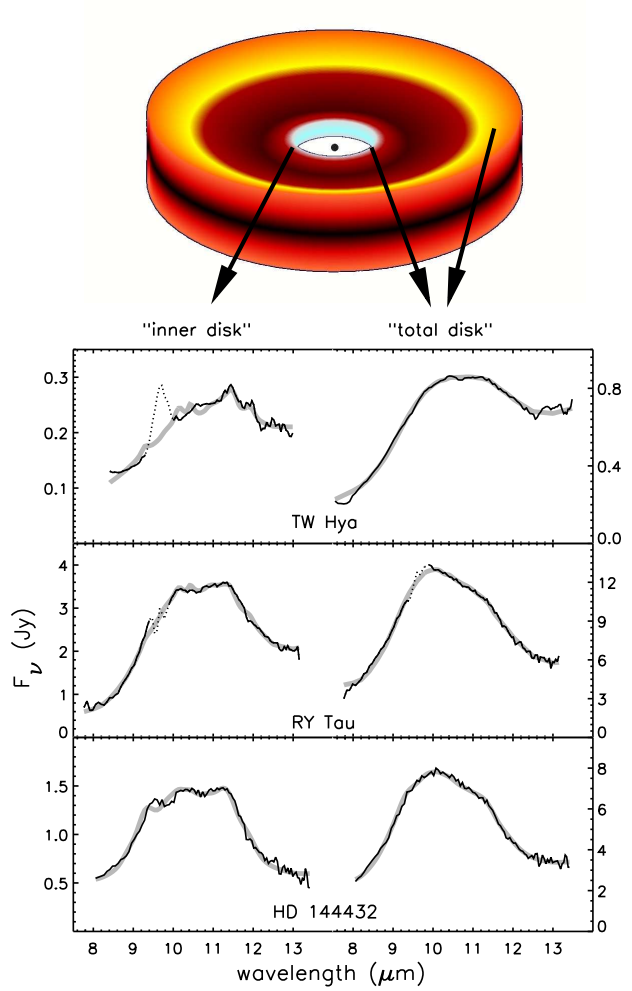

Fig. 5.— Evidence for radial changes of dust composition in the circumstellar disks of young stars. Infrared spectra of the inner ≈ 1–2 AU are shown in the left panels, and of the total disk (≈ 1–20 AU) in the right panels. The different shapes of the silicate emission lines testify that in the inner disk – as probed by the interferometric measurement – the fraction of crystalline particles is high while the fraction of small amorphous particles is significantly reduced. TW Hya (0.3 $L_\odot$) and RY Tau (18 $L_\odot$) approximately bracket the luminosity range of T Tauri stars, the 10 $L_\odot$ HAe star HD 144432 (from *van Boekel et al.*, 2004) is included to emphasize the similarity between these two classes of young objects. Credit: Roy van Boekel.

may however be addressed in follow-up observations of this and similar objects, perhaps exploiting enhanced spectral resolution modes (up to $R = 10000$ possible with VLTI/AMBER) and closure phase capabilities.

Quirrenbach et al. (2006) have also presented preliminary VLTI/MIDI results of rich spectral content for the wind environment in another high luminosity YSO, MWC 349–A. The general shape of the N-band spectrally resolved visibilities is consistent with disk emission, as in the *Leinert et al.* (2004) results (Section 3.1). In addition, the visibility spectrum contains unprecedented richness, displaying over a dozen lines corresponding to wind emission in forbidden ([NeII], [ArIII], [SIV]) and H recombination lines. The relative amplitudes of the visibilities measured in the continuum and in the lines indicate that the forbidden line region is larger than the dust disk, and that the recombination region is smaller than the dust disk (at least along some directions). Moreover, differential phases measured with respect to the continuum also display structure as a function of wavelength, showing clear phase shifts that encode information about the relative locations of the emitting regions for the strongest emission lines.

4.2 Multiplicity and Stellar Masses

Most young (and main sequence) stars are members of multiple systems, likely as a result of the star formation process itself (see the chapters by *Goodwin et al.* and by *Duchene et al.*). The measurement of the physical orbits of stars in multiple systems provide the only direct method for measuring stellar masses, a fundamental stellar parameter. In turn, by placing stars with measured masses in an HR-diagram, models of stellar structure and evolution can be critically tested and refined, provided the mass measurements have sufficient accuracy (see the chapter by *Mathieu et al.*). Generally speaking, dynamical and predicted masses agree well for $1-10 M_\odot$ stars in the main sequence. However, fundamental stellar properties are much less well known for pre-main sequence (PMS) stars, particularly of low-mass (*Hillenbrand and White*, 2004), and call for mass measurements with better than 10% accuracy.

Optical interferometers can spatially resolve close binaries (having separations of order ~ 1 mas, or 1/10ths AU at 150 pc), and establish the apparent astrometric orbits, most notably its inclination (for eclipsing binaries, the inclination is naturally well constrained). In combination with radial velocity measurements using Doppler spectroscopy, a full solution for the physical orbit and the properties of the system can then be obtained, in particular the individual stellar masses and luminosities. This method has proved very fruitful for critical tests of stellar models for non-PMS stars (e.g., *Boden et al.*, 2005a), however few simultaneous radial velocity and astrometric measurements exist for PMS stars.

Boden et al. (2005b) performed the first direct measurement of PMS stellar masses using optical interferometry, for the the double-lined system HD 98800–B (a pair in a quadruple system located in the TW Hya association). Using observations made at the KI and by the Fine Guidance Sensors aboard the Hubble Space Telescope, and in combination with radial velocity measurements, these authors establish a preliminary orbit which allowed determination of the (sub-solar) masses of the individual components with 8% accuracy. Comparison with stellar models indicate the need for sub-solar abundances for both components, although stringent tests of competing models will only become possible when more observations improve the orbital phase coverage and thus the accuracy of the stellar masses derived.

Naturally, disk phenomena (circumstellar and/or cir-

cumbinary) are also often observed in young multiple systems (see the chapter by *Monin et al.*); and a number of recent observations also address this interesting and more complicated situation. Indeed, successful modelling of the individual HD 98800–B components by *Boden et al.* (2005b) requires a small amount of extinction (A_V = 0.3) toward the B–components, not required toward the A–components, and possibly due to obscuration by circumbinary disk material around the B system (originally hypothesized by *Tokovinin*, 1999). As another example, based on a low-level oscillation in the visibility amplitude signature in the PTI data for FU Ori, *Malbet et al.* (2005) claim the detection of an off-centered spot embedded in the disk that could be physically interpreted as a young stellar or proto-planetary companion (located at $\sim$ 10 AU), and possibly be at the origin of the FU Ori outburst itself.

As noted by *Mathieu* (1994), spectroscopic detection of radial velocity changes is challenging in the presence of strong emission lines, extreme veiling or rapid rotation, all of which are common in PMS stars. Therefore, imaging techniques are unique discovery tools for PMS multiples. For the closest systems in particular, interferometric techniques can reveal companions with separations $\sim \times 10$ smaller than single-aperture techniques (e.g., speckle or adaptive optics). Therefore, the increasing number of new detections will also add an important new sample to statistical studies aimed at determining the multiplicty fraction for young stars, its dependence on separation, stellar properties and evolutionary status, and implications for circumstellar disk survival in close binary environments.

5. SUMMARY AND OPEN QUESTIONS

5.1. Summary

Long-baseline interferometers operating at near and mid-infrared wavelengths have spatially resolved the circumstellar emission of a large number of YSOs of various types (60 objects published to date), most within the last few years. While the new observables are relatively basic in most cases (broadband visibility amplitudes), they have provided fundamentally new direct information (characteristic sizes and crude geometry), placing powerful new constraints on the nature of these circumstellar environments. In addition, more powerful observational capabilities combining high spatial resolution and spectral resolution have just begun to deliver their potential as unique tools to study YSO environments in exquisite detail and to provide breakthrough new molecular and kinematic data.

The principal well-established observational facts may be summarized as follows:

(i) For HAe, late HBe and T Tauri objects the measured NIR characteristic sizes are much larger (by factors of $\sim 3-7$) than predicted by previous-generation models which had been reasonably successful at reproducing the unresolved spectro-photometry. In particular, the measured sizes are larger than initial inner dust hole radii estimates and than magnetospheric truncation radii. The measured NIR sizes strongly correlate with the central luminosity, and the empirical NIR size *vs.* luminosity relation (Fig. 2) suggests that the NIR emission is located at radii corresponding to sublimation radii for dust directly heated by the central star. These measurements have motivated in part the development of a new class of models for the origin of the NIR disk emission (the "puffed-up" inner wall models) which not only provide qualitative agreement with the interferometer data, but also solves the SED "NIR bump" problem for HAe objects.

(ii) Some (but not all) of the earliest-type HBe objects are different than the later types in terms of their NIR size-scales. Many are inferred to have relatively small inner dust holes in better agreement with the classical disk picture, while others have larger NIR sizes consistent with the inner rim models (or perhaps even larger than predictions of either competing disk model, e.g., LkHα 101).

(iii) FU Ori, the prototype for the sub-class of YSOs expected to have disks which dominate the total luminosity, is well described by the canonical model temperature law (based on modelling the NIR interferometry data and SED). For other systems in this class however, the observations reveal more complexity and the need for data at multiple baselines and wavelengths in order to discriminate between competing scenarios.

(iv) Young disks have also been resolved at MIR wavelengths, revealing characteristic sizes which correlate with red color (IRAS $12-25\,\mu m$). This link appears to support an SED-based classification based on the degree of outer disk flaring, although the current sample of measured MIR sizes is too small to extract a firm conclusion.

(v) Spectrally-resolved MIR visibilities have emerged as a powerful tool to probe the dust minerology in young disks. Silicate dust appears to be deficient in small ($0.1\,\mu m$) amorphous grains and more crystalline (less amorphous) close to the central star when compared to the disk as a whole.

(vi) The power of spectrally-resolved visibilities, both NIR and MIR, has also been dramatically demonstrated in observations of lines corresponding to the gas component in wind phenomena associated with high-mass young stars.

(vii) Masses have been measured for young stars for the first time using interferometric techniques, in combination with spectroscopic radial velocity techniques; and a number of systems are being pursued with the primary goal of providing useful constraints to state of the art models of stellar structure and evolution.

5.2. Open Questions

The new interferometric observations have allowed a direct view of the inner regions of YSO accretion disks for the first time. While this work has motivated significant additions to our standard picture of these regions (such as the puffed-up inner rim and spatially-varying dust properties), continued theoretical development will require more

sophisticated and complete interferometry data. In this section, we outline the most pressing un-resolved issues exposed by the progress describe above:

(i) A disk origin for the resolved NIR emission has not been unambiguously established. Most notably, *Vincovik et al.* (2006) (and references therein) consider that the remaining scatter in the size-luminosity relation for HAeBe objects indicates that the bright-ring model does not adequately describe all the objects with a uniform set of parameters, and propose instead a disk plus compact halo model, where the resolved NIR emission in fact corresponds to the compact halo component. Because the halo need not be spherically symmetric, the elongations detected at the PTI do not rule it out. Effectively re-igniting the *disk vs. envelope* debate of the previous decade (see e.g., *Natta et al.*, 2000), *Vincovik et al.* (2006) also show that this model equivalently reproduces the SED, including the NIR bump.

(ii) The detailed properties of the putative puffed-up inner rim remain to be established. Assumptions about the grain size and density directly impact the expected rim location (dust sublimation radius), and based on size comparisons (Fig. 2) current observations appear to indicate that a range of properties may be needed to explain all disks, particularly among the T Tauri objects. HAe objects have NIR sizes consistent with optically thin dust and relatively large grains ($\sim 1\,\mu m$). The lowest luminosity T Tauri objects however favor either optically thick dust or smaller grains, or a combination of both. Currently however, the T Tauri sample is still small, several objects are barely resolved, and part of the scatter could be due to unreliable SED decomposition due to photometric variability and uncertain stellar properties. Detailed modelling of individual objects and crucial supporting observations such as infrared veiling (to directly establish the excess flux) are needed to help resolve these uncertainties.

(iii) Using IR spectroscopy, it has been established that the *gas* in young disk systems extends inward of the interferometrically deduced inner dust radii (see the chapter by *Najita et al.*). Whether or not magnetospheric accretion theories can accomodate these observations remains to be explored. We note that current interpretations of the CO spectroscopy do not take into account the inner rim, relying instead on previous-generation models that have been all but ruled out for the inner few AU. Finally, effects of NIR emission by gas in the inner disk, both on the measured visibilities and on the SED decomposition (both of which affect the inferred NIR sizes), need to be quantified in detail on a case-by-case basis.

(vi) Large scale ($\sim 50 - 1000$ mas) "halos" contributing small but non-negligible NIR flux ($\sim$ 10%) are often invoked as an additional component needed to satisfactorily model some YSO disks (e.g., the FU Orionis objects, or most recently in the IOTA-3T HAeBe sample of *Monnier et al.*, 2006, in preparation). The origin of this halo material is however unclear, as is its possible connection with the compact halos proposed by *Vincovik et al.* (2006). The observational evidence should motivate further work on such multi-component models.

(vii) Late (HAe, late HBe) and early HBe systems appear to have different NIR scale properties (see Section 2.1), although there are notable exceptions, and the sample is small. Differences between these types have also been noted in terms of their mm emission (absent in most early HBe, in contrast to the late Herbig and T Tauri objects), perhaps due to outer-disk photoevaporation (*Hollenbach et al.*, 2000, and see also the chapter by *Dullemond et al.*). Whether the observed differences in inner disk structure are due to different accretion mechanisms (disk accretion vs. magnetospheric accretion) or to gas opacity effects remains to be investigated.

(viii) Do all FU Orionis objects conform to the canonical accretion disk model? If so, the additional question arises as to why their temperature structure would be that simple. Their light curves are fading, indicating a departure from a steady-state disk. Indeed, the high outburst accretion rates are expected to decay, and to do so in a radially dependent manner, leading to non-standard temperature laws. First observations using VLTI/MIDI do not indicate a simple connection between the NIR and MIR radial disk structure. Indeed, fitting the MIR visibilities and SED of V1647 Ori requires a very flat $q = -0.5$ radial temperature exponent (*Ábrahám et al.*, 2006), and preliminary analysis of FU Ori itself (*Quanz*, 2006) indicates that the model constructed by *Malbet et al.* (2005) to fit the NIR AMBER data and the SED does not reproduce (over-estimates) the measured N-band visibilities.

(ix) The overall disk structure needs to be secured. While the NIR data probe primarily the hottest dust, the MIR observations are sensitive to a wider range of temperatures. Given the complexity of the disk structure under consideration, correctly interpreting the MIR and NIR data for the same object is proving challenging. Assumptions made for modelling the NIR data, the MIR dust features, and CO line profiles are generally not consistent with each other. Excitingly, the joint modeling of near and mid-IR high resolution data can yield the temperature profile of the disk surface layers.

(x) Chemical models of proto-planetary disks, including the effects of radial transport and vertical mixing, must explain the observed dust mineralogy, and the differences seen among different types of objects. Also, we note that the effect of the inner rim (which contributes $\sim 20\%$ of the MIR flux – see Fig. 3) on the interpretation of the observed Silicate features and inferred mineralogy gradients must be assesed in detail.

6. FUTURE PROSPECTS

This review marks the maturation of two-telescope (single-baseline) observations using infrared interferometry. However, much more information is needed to seriously constrain the next generation of models (and the proliferating parameters) and to provide reliable density and temperature profiles as initial conditions for planet formation

theories. Fortunately, progress with modern interferometers continues to accelerate and will provide the unique new observations that are needed. In this section, we briefly discuss the expected scientific impact on yet-unexplored areas that can be expected from longer baselines, multi-wavelength high-resolution data, spectral line and polarization capabilities, closure phase data and aperture synthesis imaging. We will end with suggestions for disk modelers who wish to prepare for the new kinds of interferometric data in the pipeline.

6.1. Detailed Disk Structure

All interferometric observations of YSO disks to date have used baselines $\lesssim 100$ meters, corresponding to angular resolution of ~ 2 and 11 milliarcsec at 2.2 and 10 microns respectively. While sufficient to resolve the overall extent of the disks, longer baselines are needed to probe the internal structure of this hot dust emission. For instance, current data can not simultaneously constrain the inner radius and thickness of the inner rim dust emission, the latter often assumed to be "thin" ($10 - 25\%$ of radius). Nor can current data independently determine the fraction of light from the disk compared to star (critical input to the models), relying instead on SED decomposition.

Longer baselines from the CHARA Interferometer (330 meters) and from VLTI Interferometer (200 meters) can significantly increase the angular resolution and allow the rim emission to be probed in detail. For instance, if the NIR emission is contained in a thin ring, as expected for "hot inner wall" models, there will be a dramatic signal in the second lobe of the interferometer visibility response. Competing "halo" models predict smoother fall-offs in brightness (and visibility) and thus new long-baseline data will provide further definitive and completely unique constraints on the inner disk structure of YSOs (first long-baseline CHARA observations of YSOs were presented by *Monnier et al.*, 2005b).

While even two-telescope visibility data provide critical constraints, ultimately we strive for aperture synthesis imaging, as routinely done at radio wavelengths. The first steps have recently been taken with closure phase results on HAeBe objects using IOTA/IONIC3 (*Millan-Gabet et al.*, 2006b; *Monnier et al.*, 2006; both in preparation). Closure phases are produced by combining light from three or more telescopes, and allow "phase" information to be measured despite atmospheric turbulence (see e.g., *Monnier*, 2000). While this phase information is essential for image reconstruction, the closure phase gives unambiguous signal of "skewed" emission, such as would arise from a flared disk viewed away from the pole. "Skew" in this context indicates a deviation from a centro-symmetric brightness.

Closure phases are interesting for measuring the vertical structure of disks. Early hot inner wall models (e.g., *Dullemond et al.*, 2001) posited vertical inner walls. Recently, the view was made more realistic by *Isella and Natta* (2005) by incorporating pressure-dependent dust sublimation temperatures to curve the inner rim away from the midplane. Closure phases can easily distinguish between these scenarios because vertical walls impose strong skewed emission when a disk is viewed at intermediate inclination angles, while curved inner walls appear more symmetric on the sky unless viewed nearly edge-on. NIR closure phase data will soon be available from IOTA/IONIC3, VLTI/AMBER and CHARA/MIRC that can be used to measure the curvature and inner rim height through model fitting of specific sources.

Aperture synthesis imaging of selected YSOs using the VLTI and CHARA arrays should also be possible within the next five years. By collecting dozens of closure phase triangles and hundreds of visibilities, simple images can be created as has been demonstrated for LkHα 101 using the aperture masking technique. First steps in this direction have been presented for the triple T Tauri system GW Ori (also believed to contain circumstellar and circumbinary disks) by *Berger et al.* (2006), who present preliminary separation vectors and the first reconstructed image of a young multiple system. Ultimately, YSO imaging will allow the first model-independent tests of disk theories; all current interpretations are wed to specific (albeit general) models and the first images may be eye-opening.

As described earlier (Section 3), it is essential to know the properties of circumstellar dust particles in YSO disks in order to interpret a broad range of observations, most especially in standard SED modelling. Interferometers can measure dust properties, such as size distribution and composition, using the combination of NIR, MIR, and polarization measurements. Efforts are being explored at the PTI, IOTA, VLTI and CHARA interferometers to measure the disk emission in linearly polarized light (see *Ireland et al.*, 2005 for similar first results for dust around AGB stars). Because scattering is heavily dependent on grain-size, the polarization-dependent size estimates at different wavelengths will pinpoint the sizes of the grains present in the inner disk.

With its nulling capability at MIR wavelengths, the KI (*Serabyn et al.*, 2004) will soon address a wide range of YSO phenomena, from spectrally resolved MIR disk structure in young disks to exo-zodiacal emission (*Serabyn et al.*, 2000), the latter being a crucial element in the selection of favorable targets for future space-based planet finding missions (e.g., Terrestrial Planet Finder/Darwin, *Fridlund*, 2003).

Proto-planets forming in circumstellar disks are expected to carve fine structure, such as gaps, opening the possibility of directly detecting this process via high dynamic range interferometric techniques (e.g., highly accurate visibility amplitude measurements). While some initial simulations are pessimistic that new interferometers can resolve such disk structures (*Wolf et al.*, 2002), it is clear that theorists have only begun to investigate the many possibilities and interferometers are gearing up to meet the necessary observational challenges ahead.

Finally, although outside the scope of this review, we point out the tremendous potential of the upcoming Atacama Large Millimiter Array (ALMA, *Wootten*, 2003). In particular, the combination of infrared, mm and sub-mm interferometry will probe the entire YSO disk at all scales.

6.2. Dynamics

New spectral line (e.g., VLTI/AMBER) capabilities have exciting applications. For instance, spectro-interferometry can measure the Keplerian rotation curves (in CO) for disks to derive dynamical masses of young stars as has been done using mm-wave interferometry (*Simon et al.*, 2000). Clearly, the potentially very powerful combination of spectroscopy and interferometry has only begun to be explored.

The dynamic time scale for inner disk material can be $\lesssim$ 1 year, thus we might expect to see changes with time. The higher the angular resolution, the greater the possibility that we can identify temporal changes in the circumstellar structures. If disk inhomogeneities are present, new measurements will discover them and track their orbital motions. Evidence of inner disk dynamics has been previously inferred from reflection nebulosity (e.g., HH 30, *Stapelfeldt et al.*, 1999) and photometric variability (e.g., *Hamilton et al.*, 2001); but only recently directly imaged at AU scales (LkHα 101, *Tuthill et al.*, 2002).

6.3. The Star - Disk - Outflow Connection

The interface between the star, or its magnetosphere, and the circumstellar disk holds the observational key into how disks mediate angular momentum transfer as stars accrete material. The relevant spatial scales (1 to few $R_\star$) may be resolvable by the longest baselines available, providing unique tests of magnetospheric accretion theories (see the chapter by *Bouvier et al.*).

In addition to being surrounded by pre-planetary disks, YSOs are often associated with outflow phenomena, including optical jets, almost certainly associated with the disk accretion process itself (see the chapter by *Bally et al.*). The precise origin of the jet phenomena is however unknown, as is the physical relation between the young star, the disk, and jets (see the chapter by *Ray et al.*). Discriminating among competing models, e.g., jets driven by external large scale magnetic fields (the "disk wind" models or stellar fields models) or by transient local disk fields, can be helped by determining whether the jets launch near the star, or near the disk. Observationally, progress depends in part on attaining sufficient spatial resolution to probe the jet launching region directly, a natural task for optical interferometers (e.g., *Thiebaut et al.*, 2003).

6.4. New Objects

Infrared interferometry can directly address important questions concerning the early evolution of high mass (O–B) protostars (see the chapter by *Cesaroni et al.* for a review of the pressing issues), and observational work in this area using infrared interferometry has just begun (with the VLTI/MIDI observations of *Quirrenbach et al.*, 2006; *Feldt et al.*, 2006). Most notably, it is not presently known what role, if any, accretion via circumstellar disks plays in the formation of high-mass stars. If present, interferometers can resolve circumstellar emission, and determine whether or not it corresponds to a circumstellar disk. Further, by studying disk properties as a function of stellar spectral type, formation timescales and disk lifetimes can be constrained.

Current studies have mainly targeted young disk systems, i.e. class II (*Adams et al.*, 1987). More evolved, class III, disks have remained thus far unexplored (the only exception being V380 Ori in *Akeson et al.*, 2005a), due to the sensitivity limitations that affected the first observations. Moreover, directly establishing the detailed disk structure of transition objects in the planet-building phase and of debris disks on sub-AU to 10s AU scales will likely be an energetic area of investigation as the field progresses towards higher dynamic range and spatial frequency coverage capabilities. First steps have been taken in this direction, with NIR observations that resolve the transition object TW Hya (*Eisner et al.*, 2006) and detect dust in the debris disk around Vega (*Ciardi et al.*, 2001; *Absil et al.*, 2006, in preparation).

Finally, we note that prospects also exist for the direct detection of exo-planets from the ground, including interferometric techniques, and we refer the reader to the chapter by *Beuzit et al.*

6.5. Comments on Modelling

A number of new physical ingredients must be introduced into current disk models in order to take advantage of interferometer data. Disk models should take into account both vertical variations (settling) and radial dust differences (processing and transport). Also, the structure of inner wall itself depends on the physics of dust destruction, and may depend on gas cooling and other physical effects not usually explicitly included in current codes. Perhaps codes will need to calculate separate temperatures for each grain size and type to accurately determine the inner rim structure. Lastly, we stress that the many free parameters in these models can only be meaningfully constrained through a data-driven approach, fitting not only SEDs (normal situation) but NIR and MIR interferometry simultaneously for many individual sources. With these new models, disk mass profiles and midplane physical conditions will be known, providing crucial information bridging the late stages of star formation to the initial conditions of planet formation.

Acknowledgments.
We thank Roy van Boekel for providing Figs. 3 and 5 and for helpful discussions. We also thank many of our colleagues for illuminating discussions while preparing this review, in particular Myriam Benisty, Jean-Philippe Berger, Andy Boden, Kees Dullemond, Josh Eisner, Lynne Hillenbrand and Andreas Quirrenbach.

REFERENCES

Ábrahám P., Kóspál Á., Kun M., Moór A. et al. (2004) *Astron. Astrophys., 428*, 89-97.

Ábrahám P., Mosoni, L., Henning Th., Kóspál Á., Leinert Ch. et al. (2006) *Astron. Astrophys., in press*.

Adams F. C., Lada C. J., and Shu F. H. (1987) *Astrophys. J., 312*, 788-806.

Akeson R. L., Ciardi D. R., van Belle G. T., Creech-Eakman M. J., and Lada E. A. (2000) *Astrophys. J., 543*, 313-317.

Akeson R. L., Ciardi D. R., van Belle G. T., and Creech-Eakman, M. J. (2002) *Astrophys. J., 566*, 1124-1131.

Akeson R. L., Boden A. F., Monnier J. D., Millan-Gabet R., Beichman C. et al. (2005a) *Astrophys. J., 635*, 1173-1181.

Akeson R. L., Walker C. H., Wood K., Eisner J. A., and Scire E. (2005b) *Astrophys. J., 622*, 440-450.

Berger J.-P., Monnier J. D., Pedretti E., Millan-Gabet R., Malbet, F. et al. (2005) in *Protostars and Planets V Poster Proceedings* `http://www.lpi.usra.edu/meetings/ppv2005/pdf/8398.pdf`

Bjorkman J. E. and Wood K. (2001) *Astrophys. J., 554*, 615-623.

Boden A. F., Torres G., and Hummel C. A. (2005a) *Astrophys. J., 627*, 464-476

Boden A. F., Torres G., and Hummel C. A. (2005b) *Astrophys. J., 627*, 464-476.

Bockelée–Morvan D., Gautier D., Hersant F., Huré, J.-M., and Robert F. (2002) *Astron. Astrophys., 384*, 1107-1118.

Casse F. and Ferreira J. (2000) *Astron. Astrophys., 353*, 1115-1128.

Chiang E. and Goldreich P. (1997) *Astrophys. J., 490*, 368.

Ciardi D. R., van Belle G. T., Akeson R. L., Thompson, R. R., Lada, E. A. et al. (2001), *Astrophys. J., 559*, 1147-1154.

Colavita M. M., Wallace J. K., Hines B. E., Gursel Y., Malbet F. et al. (1999) *Astrophys. J., 510*, 505-521.

Colavita M. M., Akeson R., Wizinowich P., Shao M., Acton S. et al. (2003) *Astrophys. J., 529*, L83-L86.

Colavita M. M., Wizinowich P. L., and Akeson R. L. (2004) in *Proceedings of the SPIE, 5491*, 454.

Clarke C. J., Gendrin A., and Sotomayor M. (2001) *Mon. Not. R. Astron. Soc.328*, 485-491.

Crovisier J., Akeson R., Wizinowich P., Shao M., Acton S. et al. (1997) *Science, 275*, 1904-1907.

D'Alessio P., Calvet N., Hartmann L., Muzerolle J., and Sitko M. (2004) in *Star Formation at High Angular Resolution, IAU Symposium*, (M. G. Burton, R. Jayawardhana, and T. L. Bourke, eds.), *221*, 403-410.

Danchi W. C., Tuthill P. G., and Monnier J. D. (2001) *Astrophys. J., 562*, 440-445.

Dominik C., Dullemond C. P., Waters L. B. F. M., and Walch S. (2003) *Astron. Astrophys., 398*, 607-619.

Dullemond C. P., Dominik C., and Natta A. (2001) *Astrophys. J., 560*, 957-969.

Dullemond C. P. and Dominik C. (2004) *Astron. Astrophys., 417*, 159-168.

Drew J., Busfield G., Hoare M. G., Murdoch K. A., Nixon C. A. et al. (1997) *Mon. Not. R. Astron. Soc., 286*, 538-548.

Eisner J. A., Busfield G., Hoare M. G., Murdoch K. A., and Nixon C. A. (2003) *Astrophys. J., 588*, 360-372.

Eisner J. A., Lane B. F., Hillenbrand L. A., Akeson R. L., and Sargent A. I. (2004) *Astrophys. J., 613*, 1049-1071.

Eisner J. A., Hillenbrand L. A., White R. J., Akeson R. L., and Sargent A. I. (2005) *Astrophys. J., 623*, 952-966.

Eisner J. A., Chiang, E. I., and Hillenbrand, L. A. (2006) *Astrophys. J., in press*.

Feldt M., Pascucci I., Chesnau O., Apai D., Henning Th. et al. (2006) in *The Power of Optical / IR Interferometry: Recent Scientific Results and 2nd Generation VLTI Instrumentation*, (F. Paresce, A. Richichi, A. Chelli, and F. Delplancke, eds.), ESO Astrophysics Symposia, Springer-Verlag, Garching.

Fridlund M. C. (2003) in *Proceedings of the SPIE*, 5491, 227.

Gail H.-P. (2004) *Astron. Astrophys., 413*, 571-591.

Garcia P. J. V., Glindeman A., Henning T., and Malbet F. (eds.) (2004) *The Very Large Telescope Interferometer – Challenges for the Future*, Astrophysics and Space Science Volume 286, Nos. 1-2, Kluwer Academic Publishers, Dordrecht.

Gil C., Malbet F., Schoeller M., Chesnau O., Leinert Ch. et al. (2006) in *The Power of Optical / IR Interferometry: Recent Scientific Results and 2nd Generation VLTI Instrumentation*, (F. Paresce, A. Richichi, A. Chelli, and F. Delplancke, eds.), ESO Astrophysics Symposia, Springer-Verlag, Garching.

Hamilton C., Herbst W., Shih C., and Ferro A. J. (2001) *Astrophys. J., 554*, L201-L204.

Hanner M. S., Lynch D. K., and Russell R. W. (1994) *Astrophys. J., 425*, 274-285.

Hale D., Bester M., Danchi W. C., Fitelson W., Hoss, S. et al. (2000) *Astrophys. J., 537*, 998-1012.

Hartmann L. and Kenyon S. J. (1985) *Astrophys. J., 299*, 462-478.

Hartmann L. and Kenyon S. J. (1996) *Ann. Rev. Astron. Astrophys., 34*, 207-240.

Hartmann L., Calvet N., Gullbring E., and D'Alessio P. (1998) *Astrophys. J., 495*, 385.

Herbig G. H., Petrov P. P., and Duemmler R. (2003) *Astrophys. J., 595*, 384-411.

Hillenbrand L. A., Strom S. E., Vrba F. J., and Keene J. (1992). *Astrophys. J., 397*, 613-643.

Hillenbrand L. A. and White R. J. (2004) *Astrophys. J., 604*, 741-757.

Hinz P. M., Hoffmann W. F., and Hora J. L. (2001) *Astrophys. J., 561*, L131-L134.

Hollenbach D., Yorke H. W., and Johnstone D. (2000) in *Protostars and Planets IV*, (Mannings, V., Boss, A. P., and Russell, S. S. eds.), pp. 401-428, Univ. of Arizona Press, Tucson.

Ireland M., Tuthill P. G., Davis J., and Tango W. (2005) *Mon. Not. R. Astron. Soc., 361*, 337-344.

Isella A. and Natta A. (2005) *Astron. Astrophys., 438*, 899-907.

Jayawardhana R., Fisher S., Hartmann L., Telesco C., Pina R. et al. (1998) *Astrophys. J., 503*, L79.

Johns-Krull C. M. and Valenti V. A. (2001) *Astrophys. J., 561*, 1060-1073.

Kemper F., Vriend W. J., and Tielens A. G. G. M. (2004) *Astrophys. J., 609*, 826-837.

Kenyon S. J. and Hartmann L. W. (1987) *Astrophys. J., 323*, 714-733.

Kenyon S. J. and Hartmann L. W. (1991) *Astrophys. J., 383*, 664-673.

Koerner D. W., Ressler M. E., Werner M. W., and Backman D. E. (1998) *Astrophys. J., 503*, L83.

Kuchner M. and Lecar M. (2002) *Astrophys. J., 574*, L87-L89.

Lachaume R., Malbet F., and Monin J.-L. (2003) *Astron. Astrophys., 400*, 185-202.

Lawson P. (ed.) (2000) *Principles of Long Baseline Interferometry*, published by National Aeronautics and Space Administration, Jet Propulsion Laboratory, California Institute of Tech-

nology, Pasadena.
Leinert Ch., Haas M., Abraham P., and Richichi A. (2001) *Astron. Astrophys., 375*, 927.
Leinert Ch. Graser U., Przygodda F., Waters L. B. F. M., Perrin G. et al. (2003) *Astrophys. Space Sci., 286*, 1, 73-83.
Leinert Ch., van Boekel R., Waters L. B. F. M., Chesneau O., Malbet F. et al. (2004) *Astron. Astrophys., 423*, 537-548.
Lin D. N. C., Bodenheimer P., and Richardson D. C. (1996) *Nature, 380*, 606-607.
Liu W. M., Hinz P. M., Meyer M. R., Mamajek E. E. et al. (2003) *Astrophys. J., 598*, L111-L114.
Liu W. M., Hinz, P. M., Hoffmann W. F., Brusa G., Miller D. et al. (2005) *Astrophys. J., 618*, L133-L136.
Lynden-Bell D. and Pringle J. E. (1974) *Mon. Not. R. Astron. Soc., 168*, 603-637.
Malbet F. and Bertout C. (1995) *Astron. Astrophys. Suppl., 113*, 369.
Malbet F., ., Berger J.-P., Colavita M. M., Koresko C. D., Beichman C. et al. (1998) *Astrophys. J., 507*, L149-L152.
Malbet F., Driebe T. M., Foy R., Fraix-Burnet D., Mathias P. et al. (2004) in *Proceedings of the SPIE, 5491*, 1722.
Malbet F., Lachaume R., Berger J.-P., Colavita M. M., di Folco, E. et al. (2005) *Astron. Astrophys., 437*, 627-636.
Malbet F., Benisty M., de Wit W. J., Kraus S., Meilland A. et al. (2006) *Astron. Astrophys., in press*.
Mathieu R. D. (1994) *Ann. Rev. Astron. Astrophys., 32*, 465-530.
McCabe C., Duchene G., and Ghez A. (2003) *Astrophys. J., 588*, 2, L113-L116.
Meeus G., Waters L. B. F. M., Bouwman J., van den Ancker M. E., Waelkens C. et al. (2001) *Astron. Astrophys., 365*, 476-490.
Millan-Gabet R., Schloerb F. P., Traub W. A., Malbet F., Berger J.-P., and Bregman, J. D. (1999) *Astrophys. J., 513*, L131-L143.
Millan-Gabet R., Schloerb F. P., and Traub W. A. (2001) *Astrophys. J., 546*, 358-381.
Millan-Gabet R., Monnier J. D., Akeson R. L., Hartmann L., Berger J.-P. et al. (2006) *Astrophys. J., in press*.
Monnier J. D. (2000) in *Principles of Long Baseline Interferometry* (Lawson P. ed.), pp. 203-226, published by National Aeronautics and Space Administration, Jet Propulsion Labratory, California Institute of Technology, Pasadena.
Monnier J. D. and Millan-Gabet R. (2002) *Astrophys. J., 579*, 694-698.
Monnier J. D. (2003) in *Reports on Progress in Physics*, *Vol. 66*, Num. 5, 789-897
Monnier J. D., Berger J.-P., Millan-Gabet R., and Ten Brummelaar T. A. (2004a) in *Proceedings of the SPIE, 5491*, 1370.
Monnier J. D., Tuthill P. G., Ireland M. J., Cohen R., and Tannirkulam A. (2004b), in *American Astronomical Society Meeting 2005*, 17.15.
Monnier J. D., Millan-Gabet R., Billmeier R., Akeson R. L., Wallace D., Berger J.-P. et al. (2005a) *Astrophys. J., 624*, 832-840.
Monnier J. D., Pedretti E., Millan-Gabet R., Berger J.-P., Traub, W. et al. (2005b) in *Protostars and Planets V Poster Proceedings* `http://www.lpi.usra.edu/meetings/ppv2005/pdf/8238.pdf`
Muzerolle J., Calvet N., Hartmann L., and D'Alessio P. (2003) *Astrophys. J., 597*, L149-L152
Muzerolle J., D'Alessio P., Calvet N., and Hartmann L. (2004) *Astrophys. J., 617*, 406-417.
Natta A., Grinin V., and Mannings V. (2000) in *Protostars and Planets IV*, (Mannings, V., Boss, A. P., and Russell, S. S. eds.), pp. 559-588, Univ. of Arizona Press, Tucson.
Natta A., Prusti T., Neri R., Wooden D., Grinin V. P. et al. (2001) *Astron. Astrophys., 371*, 186-197.
F. Paresce, A. Richichi, A. Chelli, and F. Delplancke (eds.) (2006) *The Power of Optical / IR Interferometry: Recent Scientific Results and 2nd Generation VLTI Instrumentation*, ESO Astrophysics Symposia, Springer-Verlag, Garching.
Perrin G. and Malbet F. (eds.) (2003) *Observing with the VLTI*, EAS Publications Series, *Volume 6*.
Quanz S. P. (2006) in *The Power of Optical / IR Interferometry: Recent Scientific Results and 2nd Generation VLTI Instrumentation*, (F. Paresce, A. Richichi, A. Chelli, and F. Delplancke, eds.), ESO Astrophysics Symposia, Springer-Verlag, Garching.
Quirrenbach A. (2001) *Ann. Rev. Astron. Astrophys., 39*, 353-401.
Quirrenbach A., Albrecht S., and Tubbs R. N. (2006) in *Stars with the B[e] phenomenon*, (Michaela Kraus and Anatoly S. Miroshnichenko, eds.), ASP Conference Series, *in press*.
Rice W. K. M., Wood K., Armitage P. J., Whitney B. A., and Bjorkman J. E. (2003) *Mon. Not. R. Astron. Soc., 342*, 79-85.
Serabyn E., Colavita M. M., and Beichman C. A. (2000) in *Thermal Emission Spectroscopy and Analysis of Dust, Disks, and Regoliths* (Michael L. Sitko, Ann L. Sprague, and David K. Lynch, eds.), *196*, pp. 357-365, ASP Conf. Series, San Francisco.
Serabyn E., Booth A. J., Colavita M. M., Creech-Eakman M. J., Crawford S. L. et al. (2004) in *Proceedings of the SPIE, 5491*, 806.
Shu F., Najita J., Ostriker E., Wilkin F., Ruden S. et al. (1994) *Astrophys. J., 429*, 781-807.
Simon M., Dutrey A., and Guilloteau S. (2000) *Astrophys. J., 545*, 1034-1043.
Stapelfeldt K., Watson A. M., Krist J. E., Burrows C. J., Crisp D. et al. (1999) *Astrophys. J., 516*, 2, L95-L98.
ten Brummelaar T. A., McAlister H. A., Ridgway S. T., Bagnuolo W. G. Jr., Turner N. H. et al. (2005) *Astrophys. J., 628*, 453-465.
Tokovinin, A. (1999) *Astron. Lett., 25*, 669-671.
Traub W. A., Berger. J.-P., Brewer M. K., Carleton N. P., Kern P. Y. et al. (2004) in *Proceedings of the SPIE, 5491*, 482.
Tuthill P., Monnier J. D., and Danchi, W. C. (2001) *Nature, 409*, 1012-1014.
Tuthill P., Monnier J. D., Danchi W. C., Hale D. D. S., and Townes C. H. (2002) *Astrophys. J., 577*, 826-838.
van Boekel R., Min M., Leinert Ch., Waters L. B. F. M., Richichi A. et al. (2004) *Nature, 432*, 479-482.
van Boekel R., Dullemond C. P., and Domink C. (2005) *Astron. Astrophys., 441*, 563-571.
Vinković D., Ivezić Ž., Jurkić T., and Elitzur M. (2006) *Astrophys. J., 636*, 348-361.
Wilkin F. P. and Akeson R. L. (2003) *Astrophys. Space Sci., 286*, 145-150.
Wootten A. (2003) in *Proceedings of the SPIE, 4837*, 110.